Journal of Sound and Vibration (2003) **259**(2), 427–443
doi:10.1006/jsvi.2002.5223, available online at http://www.idealibrary.com on IDEAL®

DYNAMICAL ANALYSIS OF A CYLINDRICAL PIEZOELECTRIC TRANSDUCER

P. Lu

Institute of High Performance Computing, Science Park II, 1 *Science Park Road,* #01-01 *The Capricorn,* 117528, *Singapore; Department of Modern Mechanics, University of Science and Technology of China, Hefei, Anhui* 230027, *People's Republic of China*

AND

K. H. Lee and S. P. Lim

Department of Mechanical Engineering, National University of Singapore, Kent Ridge, 119260, *Singapore*

(*Received* 5 *November* 2001, *and in final form* 20 *March* 2002)

In the present paper, the vibration of a cylindrical piezoelectric transducer induced by applied voltage, which can be used as the stator transducer of a cylindrical micromotor, is studied based on shell theory. The transducer is modelled as a thin elastic cylinder. The properties of the vibration modes of the transducer, such as mode frequencies and amplitude ratios of the mode shapes, are determined following Galerkin method. The response of the transducer under the four electric sources with 90° phase difference is then obtained by the modal summation method. With the results, the performance of the transducer under the electric sources can be estimated. The present work provides a general and precise theoretical modelling on the dynamical movement of the transducer.

1. INTRODUCTION

Closed circular cylindrical shell type piezoelectric transducers have been widely used in electromechanical devices. One of the successful applications is in the development of cylindrical-type ultrasonic micromotors [1]. The key component of the motors is a filmed or bulk piezoelectric tube called cylindrical stator transducer, as shown in Figure 2. It consists of a piezoceramic tube, four equal strip electrodes, where the electric wires are connected. The poling direction of the cylinder is in the thickness direction. When two opposite electric sources with applied frequency, which can excite fundamental bending mode of the cylinder, are connected to one pair of the electrodes facing each other, the bending vibration of the stator transducer is generated by the piezoelectric length-extensional effect. By applying four such electrical sources with 90° phase difference to each other simultaneously, the rotation mode of the stator transducer is excited, and a one-wavelength travelling wave is generated on the end surfaces of the stator, which drives the rotors in contact with the transducer by frictional forces. The motion principle of the motor is briefly shown in Figure 1.

Although the cylindrical ultrasonic micromotors have been investigated for many years, most of the efforts are essentially experimental. Theoretical modelling seems to lag behind

0022-460X/02/$35.00

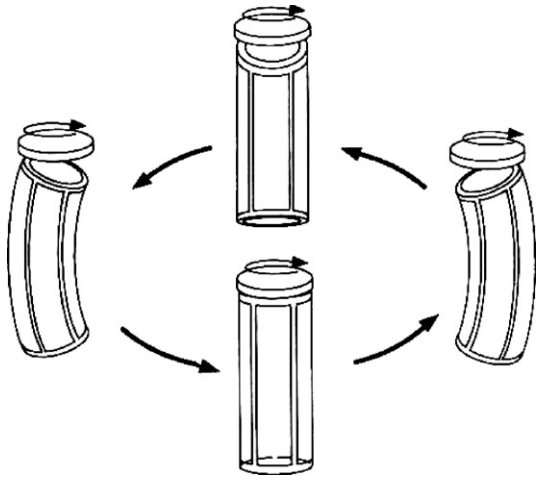

Figure 1. Principle of cylindrical ultrasonic micromotor [1].

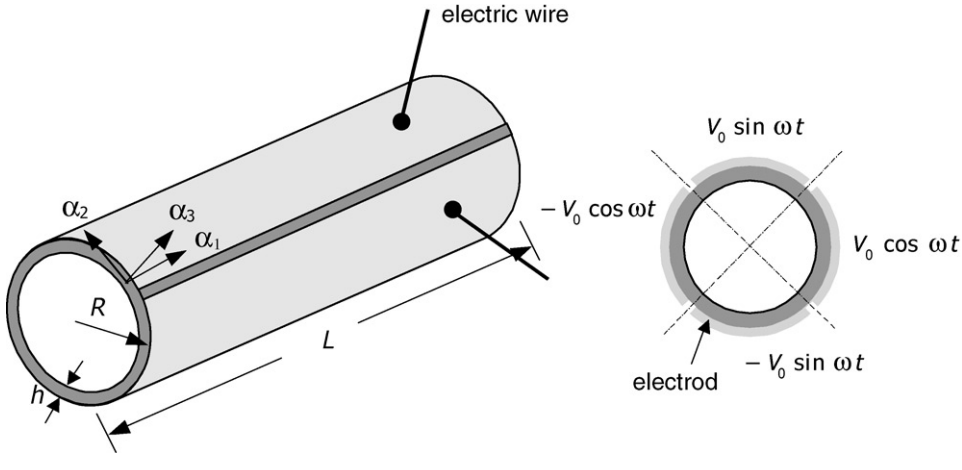

Figure 2. A radially polarized piezoelectric circular cylindrical transducer.

the experiments. The existing work in the literature is based on simple beam bending model [1, 2]. Due to restriction of the one-dimensional model, the dynamical characteristics of the motors cannot be well predicted. Therefore, it is necessary to construct more reasonable model for the cylindrical-type motors.

In the present study, the vibration of the cylindrical stator transducer of the motor is addressed. For simplicity, the contact forces between the stator and the rotor are not considered. The stator transducer is modelled as a thin closed cylindrical shell. The applied electric sources are treated as equivalent forces acting on the cylinder. To solve the shell equations, the form of the dynamic displacement components of the cylinder model is assumed based on the motion principle of the motor, and Galerkin method is applied to obtain the approximate dynamic characteristics. With the analysis, the mode shapes, the resonance frequencies, the vibration amplitudes, and the performance of the cylindrical transducer can be estimated.

2. EQUATIONS OF MOTION

A piezoelectric cylindrical transducer closed in the α_2 direction is shown in Figure 2. The thickness, length, and mean radius of the cylinder are denoted by h, L, and R respectively. The transducer can be defined by cylindrical co-ordinate system with α_1-, α_2-, and α_3- axis, in which α_1 defines the longitudinal direction (length), α_2 the circumferential direction, and α_3 the transverse direction.

For the thin piezoelectric shell poled in radial direction, only electric field E_3 along the thickness direction is considered. For the applied voltage V, the electric field E_3 can be expressed as [3]

$$E_3 = -\frac{V(t)}{h} F(\alpha_1, \alpha_2), \tag{1}$$

where $F(\alpha_1, \alpha_2)$ designates the effective surface electrode, that is, $F(\alpha_1, \alpha_2) = 1$, if (α_1, α_2) is covered by effective surface electrode and $F(\alpha_1, \alpha_2) = 0$, if (α_1, α_2) is not covered by the effective surface electrode. For the piezoelectric transducer shown in Figure 2, the four electrode dimensions can be defined as

$$\begin{aligned} &0 < \alpha_1 < L, \qquad \theta_{k1} < \alpha_2 < \theta_{k2}, \\ &\theta_{k1} = -\frac{\pi}{4} + \frac{\pi}{2}(k-1), \qquad \theta_{k2} = \frac{\pi}{4} + \frac{\pi}{2}(k-1), \quad k = 1, 2, 3, 4. \end{aligned} \tag{2}$$

Therefore, $F(\alpha_1, \alpha_2)$ can be written as

$$F(\alpha_1, \alpha_2) = [\mathrm{H}(\alpha_1) - \mathrm{H}(\alpha_1 - L)][\mathrm{H}(\alpha_2 - \theta_{k1}) - \mathrm{H}(\alpha_2 - \theta_{k2})], \tag{3}$$

where $\mathrm{H}(x - x_0)$ is the Heaviside step function, which equals 1 if $x > x_0$ and equals 0 if $x < x_0$. The voltage, V, applied at the different electrode has different time function, as shown in Figure 2.

The actuator equations for the piezoelectric cylindrical shell expressed in displacements u_1, u_2 and u_3 under the applied voltage can be written as [4]

$$\begin{aligned} &\frac{\partial N_{11}^m}{\partial \alpha_1} + \frac{1}{R}\frac{\partial N_{21}^m}{\partial \alpha_2} - \rho h \ddot{u}_1 = \frac{\partial N_{11}^e}{\partial \alpha_1}, \\ &\frac{\partial N_{12}^m}{\partial \alpha_1} + \frac{1}{R}\left(\frac{\partial N_{22}^m}{\partial \alpha_2} + \frac{\partial M_{12}^m}{\partial \alpha_1} + \frac{1}{R}\frac{\partial M_{22}^m}{\partial \alpha_2}\right) - \rho h \ddot{u}_2 = \frac{1}{R}\frac{\partial N_{22}^e}{\partial \alpha_2} + \frac{1}{R^2}\frac{\partial M_{22}^e}{\partial \alpha_2}, \\ &\frac{\partial^2 M_{11}^m}{\partial \alpha_1^2} + \frac{2}{R}\frac{\partial^2 M_{21}^m}{\partial \alpha_1 \partial \alpha_2} + \frac{1}{R^2}\frac{\partial^2 M_{22}^m}{\partial \alpha_2^2} - \frac{N_{22}^m}{R} - \rho h \ddot{u}_3 = \frac{\partial^2 M_{11}^e}{\partial \alpha_1^2} + \frac{1}{R^2}\frac{\partial^2 M_{22}^e}{\partial \alpha_2^2} - \frac{N_{22}^e}{R}. \end{aligned} \tag{4}$$

The equations are obtained based on thin shell theory, and the effects of shear deformation and rotary inertia are not included. In equation (4), the terms with the superscript m are mechanical related forces, while the terms with the superscript e are electric related forces. With Love's simplifications, the strain–displacement relations can be expressed as

$$S_{11} = S_{11}^0 + \alpha_3 \kappa_{11}, \quad S_{22} = S_{22}^0 + \alpha_3 \kappa_{22}, \quad S_{12} = S_{12}^0 + \alpha_3 \kappa_{12}, \tag{5}$$

where

$$\begin{aligned} &S_{11}^0 = \frac{\partial u_1}{\partial \alpha_1}, \quad S_{22}^0 = \frac{1}{R}\frac{\partial u_2}{\partial \alpha_2} + \frac{u_3}{R}, \quad S_{12}^0 = \frac{1}{R}\frac{\partial u_1}{\partial \alpha_2} + \frac{\partial u_2}{\partial \alpha_1}, \\ &\kappa_{11} = -\frac{\partial^2 u_3}{\partial \alpha_1^2}, \quad \kappa_{22} = \frac{1}{R^2}\left(\frac{\partial u_2}{\partial \alpha_2} - \frac{\partial^2 u_3}{\partial \alpha_2^2}\right), \quad \kappa_{12} = \frac{1}{R}\left(\frac{\partial u_2}{\partial \alpha_1} - 2\frac{\partial^2 u_3}{\partial \alpha_1 \partial \alpha_2}\right). \end{aligned} \tag{6}$$

In equation (4), mechanical membrane forces N_{ij}^m and bending moments M_{ij}^m are given by

$$\begin{aligned} N_{11}^m &= K(S_{11}^0 + \mu S_{22}^0), \quad N_{22}^m = K(S_{22}^0 + \mu S_{11}^0), \quad N_{12}^m = \frac{K(1-\mu)}{2} S_{12}^0, \\ M_{11}^m &= D(\kappa_{11} + \mu\kappa_{22}), \quad M_{22}^m = D(\kappa_{22} + \mu\kappa_{11}), \quad M_{12}^m = \frac{D(1-\mu)}{2}\kappa_{12}, \end{aligned} \tag{7}$$

where $K = Eh/(1-\mu^2)$ is the membrane stiffness and $D = Eh^3/[12(1-\mu^2)]$ is the bending stiffness. The electric membrane forces N_{ij}^e and bending moments M_{ij}^e can be obtained as

$$N_{11}^e = N_{22}^e = \int_{\alpha_3} e_{31} E_3 \, \mathrm{d}\alpha_3, \qquad M_{11}^e = M_{22}^e = \int_{\alpha_3} e_{31} E_3 \alpha_3 \, \mathrm{d}\alpha_3, \tag{8}$$

where e_{31} is the transverse piezoelectric stress constant. According to equation (1), it can be further expressed as

$$N_{11}^e = N_{22}^e = -e_{31} V(t) F(\alpha_1, \alpha_2), \qquad M_{11}^e = M_{22}^e = 0. \tag{9}$$

By substituting equations (5)–(9) into equation (4), the actuator equations can be expressed based on the displacements u_i as

$$L_{ij}(u_j) - \rho h \ddot{u}_i = q_i, \quad i,j = 1,2,3, \tag{10}$$

where the differential operators $L_{ij}(\,\cdot\,)$ are given by

$$\begin{aligned} L_{11} &= K\frac{\partial^2}{\partial\alpha_1^2} + \frac{K(1-\mu)}{2}\frac{1}{R^2}\frac{\partial^2}{\partial\alpha_2^2}, \quad L_{12} = \frac{K(1+\mu)}{2}\frac{1}{R}\frac{\partial^2}{\partial\alpha_1\partial\alpha_2}, \quad L_{21} = L_{12}, \\ L_{22} &= \left(K + \frac{1}{R^2}D\right)\left(\frac{1-\mu}{2}\frac{\partial^2}{\partial\alpha_1^2} + \frac{1}{R^2}\frac{\partial^2}{\partial\alpha_2^2}\right), \quad L_{13} = K\mu\frac{1}{R}\frac{\partial}{\partial\alpha_1}, \\ L_{23} &= -D\frac{1}{R^2}\frac{\partial}{\partial\alpha_2}\left(\frac{\partial^2}{\partial\alpha_1^2} + \frac{1}{R^2}\frac{\partial^2}{\partial\alpha_2^2}\right) + K\frac{1}{R^2}\frac{\partial}{\partial\alpha_2}, \quad L_{31} = -L_{13}, \quad L_{32} = -L_{23}, \\ L_{33} &= -D\left(\frac{\partial^4}{\partial\alpha_1^4} + \frac{2}{R^2}\frac{\partial^4}{\partial\alpha_1^2\partial\alpha_2^2} + \frac{1}{R^4}\frac{\partial^4}{\partial\alpha_2^4}\right) - K\frac{1}{R^2}, \end{aligned} \tag{11}$$

and

$$\begin{aligned} q_1 &= \frac{\partial N_{11}^e}{\partial\alpha_1} = -e_{31} V(t)[\delta(\alpha_1) - \delta(\alpha_1 - L)][\mathrm{H}(\alpha_2 - \theta_{k1}) - \mathrm{H}(\alpha_2 - \theta_{k2})], \\ q_2 &= \frac{1}{R}\frac{\partial N_{22}^e}{\partial\alpha_2} = -\frac{e_{31}}{R} V(t)[\mathrm{H}(\alpha_1) - \mathrm{H}(\alpha_1 - L)][\delta(\alpha_2 - \theta_{k1}) - \delta(\alpha_2 - \theta_{k2})], \\ q_3 &= -\frac{N_{22}^e}{R} = \frac{e_{31}}{R} V(t)[\mathrm{H}(\alpha_1) - \mathrm{H}(\alpha_1 - L)][\mathrm{H}(\alpha_2 - \theta_{k1}) - \mathrm{H}(\alpha_2 - \theta_{k2})], \end{aligned} \tag{12}$$

where $\delta(x)$ is the Dirac delta function obtained by the derivative of the Heaviside step function. q_i are the exciting force generated by the electric source.

3. APPROXIMATE SOLUTIONS

As it is known, the transducer is excited under fundamental bending mode dominated vibration during operation of the cylindrical micromotor. This understanding can help us to simplify the treatment. Based on the analysis in reference [2], the displacements u_i of the

cylindrical transducer may be written in the form

$$\begin{aligned} u_1(\alpha_1,\alpha_2,t) &= -C_1 R W'(\alpha_1)\cos(\omega t-\alpha_2),\\ u_2(\alpha_1,\alpha_2,t) &= C_2 W(\alpha_1)\sin(\omega t-\alpha_2),\\ u_3(\alpha_1,\alpha_2,t) &= C_3 W(\alpha_1)\cos(\omega t-\alpha_2), \end{aligned} \tag{13}$$

where $W(\alpha_1)$ is the fundamental bending mode shape of a transversely vibrating beam, which can represent the behaviour of a transversely vibrating cylinder with similar boundary conditions [5], and C_1, C_2 and C_3 are the constants related to the amplitude components, which can be determined by using the shell equations (10). For the transverse vibration of the cylinder-type transducer with free boundary conditions, the corresponding beam function $W(\alpha_2)$ is given in equation (67).

It is noted from equation (13) that the displacements u_i can be expressed by the superposition of two vibrations perpendicular to each other, which are excited by two electrical sources with 90° phase difference. By defining these two vibrations

$$u_i^c(\alpha_1,\alpha_2,t) = U_i^c\cos\omega t, \quad u_i^s(\alpha_1,\alpha_2,t) = U_i^s\sin\omega t \tag{14}$$

with the mode shapes

$$U_1^c = C_1[-RW'(\alpha_1)\cos\alpha_2], \quad U_2^c = C_2[-W(\alpha_1)\sin\alpha_2], \quad U_3^c = C_3 W(\alpha_1)\cos\alpha_2 \tag{15a}$$

and

$$U_1^s = C_1[-RW'(\alpha_1)\sin\alpha_2], \quad U_2^s = C_2[W(\alpha_1)\cos\alpha_2], \quad U_3^s = C_3 W(\alpha_1)\sin\alpha_2, \tag{15b}$$

respectively, the displacements u_i can be further written as

$$u_i(\alpha_1,\alpha_2,t) = u_i^c(\alpha_1,\alpha_2,t) + u_i^s(\alpha_1,\alpha_2,t). \tag{16}$$

As shown in Figure 2, the vibration u_i^c is excited by the voltages $V_0\cos\omega t$ and $-V_0\cos\omega t$, respectively, applied at the two electrodes facing each other, while the vibration u_i^s is excited by the voltages $V_0\sin\omega t$ and $-V_0\sin\omega t$, respectively, applied at another pair of electrodes. It can be seen that these two vibrations have same dynamic characteristics except the 90° phase difference. Therefore, we can take either one of the vibrations to derive the dynamic characteristics.

3.1. EIGENSOLUTIONS

The vibrations described above can be solved following the Galerkin method [5]. For eigenvalue analysis of the problem, external electric excitations are set to be zero, e.g., $q_i = 0$. By substituting u_i^c or u_i^s into the shell equations (10), and by applying Galerkin's method, one has

$$\begin{aligned} &\int_0^L\int_0^{2\pi}[L_{11}(U_1^\varsigma)+L_{12}(U_2^\varsigma)+L_{13}(U_3^\varsigma)+\rho h\omega^2 U_1^\varsigma]U_1^\varsigma R\,\mathrm{d}\alpha_2\,\mathrm{d}\alpha_1 = 0,\\ &\int_0^L\int_0^{2\pi}[L_{21}(U_1^\varsigma)+L_{22}(U_2^\varsigma)+L_{23}(U_3^\varsigma)+\rho h\omega^2 U_2^\varsigma]U_2^\varsigma R\,\mathrm{d}\alpha_2\,\mathrm{d}\alpha_1 = 0,\\ &\int_0^L\int_0^{2\pi}[L_{31}(U_1^\varsigma)+L_{32}(U_2^\varsigma)+L_{33}(U_3^\varsigma)+\rho h\omega^2 U_3^\varsigma]U_3^\varsigma R\,\mathrm{d}\alpha_2\,\mathrm{d}\alpha_1 = 0, \end{aligned} \tag{17}$$

where the differential operators L_{ij} are given in equation (11). Since the use of the mode shape functions U_i^c or U_i^s can reach same eigenvalue results, the superscript c or s in equation (17) has been represented by the notation ς. By substituting equation (15a) or

(15b) into equation (17) and performing the integrations, we obtain the equations

$$\begin{bmatrix} \rho h\omega^2 + k_{11} & k_{12} & k_{13} \\ k_{21} & \rho h\omega^2 + k_{22} & k_{23} \\ k_{31} & k_{32} & \rho h\omega^2 + k_{33} \end{bmatrix} \begin{Bmatrix} C_1 \\ C_2 \\ C_3 \end{Bmatrix} = \mathbf{0}, \tag{18}$$

where

$$\begin{gathered} k_{11} = K\left(I_3 - \frac{1-\mu}{2R^2}\right), \quad k_{12} = K\frac{1+\mu}{2R^2}, \quad k_{13} = -K\frac{\mu}{R^2}, \quad k_{21} = -K\frac{1+\mu}{2}I_1, \\ k_{22} = \left(K + \frac{D}{R^2}\right)\left(\frac{1-\mu}{2}I_1 - \frac{1}{R^2}\right), \quad k_{23} = -\frac{D}{R^2}I_1 + \frac{1}{R^2}\left(K + \frac{D}{R^2}\right), \\ k_{31} = K\mu I_1, \quad k_{32} = k_{23}, \quad k_{33} = D\left(\frac{2}{R^2}I_1 - I_2\right) - \frac{1}{R^2}\left(K + \frac{D}{R^2}\right), \end{gathered} \tag{19}$$

and

$$\begin{gathered} I_1 = \int_0^L (\mathrm{d}^2 W/\mathrm{d}\alpha_1^2) W \,\mathrm{d}\alpha_1 / \int_0^L W^2 \mathrm{d}\alpha_1, \quad I_2 = \int_0^L (\mathrm{d}^4 W/\mathrm{d}\alpha_1^4) W \,\mathrm{d}\alpha_1 / \int_0^L W^2 \,\mathrm{d}\alpha_1, \\ I_3 = \int_0^L (\mathrm{d}^3 W/\mathrm{d}\alpha_1^3)(\mathrm{d}W/\mathrm{d}\alpha_1) \,\mathrm{d}\alpha_1 / \int_0^L (\mathrm{d}W/\mathrm{d}\alpha_1)^2 \mathrm{d}\alpha_1. \end{gathered} \tag{20}$$

Since the integrated functions in integrals (20) are related to the fundamental mode shape of beam function, the integrals can be further simplified. Making use of the fact that for the beam functions

$$\frac{\mathrm{d}^4 W(\alpha_1)}{\mathrm{d}\alpha_1^4} = (\eta/L)^4 W(\alpha_1), \tag{21}$$

where η are the roots of the beam eigenvalue problem, the results of equation (20) can be applied to various boundary conditions. By examining the properties of the mode shape $W(\alpha_1)$, the ratios of the integrals can be approximately expressed as

$$I_1 \cong -(\eta/L)^2, \quad I_2 = (\eta/L)^4, \quad I_3 \cong -(\eta/L)^2. \tag{22}$$

By setting the determinant of the coefficient matrix in equation (18) to be zero, the characteristic equation of equation (18) is given as

$$\omega^6 + a_1\omega^4 + a_2\omega^2 + a_3 = 0, \tag{23}$$

where

$$\begin{gathered} a_1 = (k_{11} + k_{22} + k_{33})/\rho h, \\ a_2 = (k_{11}k_{22} + k_{22}k_{33} + k_{33}k_{11} - k_{12}k_{21} - k_{23}k_{32} - k_{31}k_{13})/(\rho h)^2, \\ a_3 = (k_{11}k_{22}k_{33} - k_{11}k_{23}k_{32} - k_{22}k_{31}k_{13} - k_{33}k_{12}k_{21} + k_{21}k_{13}k_{32} + k_{31}k_{12}k_{23})/(\rho h)^3. \end{gathered} \tag{24}$$

Solving the characteristic equation (23), three frequencies are obtained as

$$\begin{gathered} \omega_1^2 = -\frac{2}{3}\sqrt{a_1^2 - 3a_2}\cos\frac{\gamma}{3} - \frac{a_1}{3}, \quad \omega_2^2 = -\frac{2}{3}\sqrt{a_1^2 - 3a_2}\cos\frac{\gamma + 2\pi}{3} - \frac{a_1}{3}, \\ \omega_3^2 = -\frac{2}{3}\sqrt{a_1^2 - 3a_2}\cos\frac{\gamma + 4\pi}{3} - \frac{a_1}{3}, \end{gathered} \tag{25}$$

where

$$\gamma = \cos^{-1}\frac{27a_3 + 2a_1^3 - 9a_1a_2}{2\sqrt{(a_1^2 - 3a_2)^3}}. \tag{26}$$

Here the frequencies correspond to the bending, longitudinal, and circumferential mode dominated vibrations of the cylinder respectively. Usually, the lowest frequency is

associated with the mode where the transverse component dominates, while the other two are associated with the mode where the in-plane longitudinal and in-plane circumferential component dominates respectively. To have the transducer under the bending mode dominated vibration, the applied frequency should be close to the frequency of bending mode.

Substituting equation (25) into equation (18), the corresponding modal amplitude ratios of the ith component frequency are obtained as

$$\begin{aligned} \bar{C}_{1i} &= \frac{C_{1i}}{C_{3i}} = -\frac{k_{13}(\rho h\omega_i^2 + k_{22}) - k_{12}k_{23}}{(\rho h\omega_i^2 + k_{11})(\rho h\omega_i^2 + k_{22}) - k_{12}k_{21}}, \\ \bar{C}_{2i} &= \frac{C_{2i}}{C_{3i}} = -\frac{k_{23}(\rho h\omega_i^2 + k_{11}) - k_{21}k_{13}}{(\rho h\omega_i^2 + k_{11})(\rho h\omega_i^2 + k_{22}) - k_{12}k_{21}}, \quad \bar{C}_{3i} = \frac{C_{3i}}{C_{3i}} = 1. \end{aligned} \tag{27}$$

Therefore, the three component modes, which are associated with the three frequencies ω_i for the selected mode shape (15a) and (15b), are given by

$$\begin{Bmatrix} U_{1i}^c \\ U_{2i}^c \\ U_{3i}^c \end{Bmatrix} = \begin{Bmatrix} -\bar{C}_{1i} RW' \cos\alpha_2 \\ -\bar{C}_{2i} W \sin\alpha_2 \\ W \cos\alpha_2 \end{Bmatrix}, \qquad \begin{Bmatrix} U_{1i}^s \\ U_{2i}^s \\ U_{3i}^s \end{Bmatrix} = \begin{Bmatrix} -\bar{C}_{1i} RW' \sin\alpha_2 \\ \bar{C}_{2i} W \cos\alpha_2 \\ W \sin\alpha_2 \end{Bmatrix}. \tag{28}$$

3.2. RESPONSE UNDER ELECTRIC SOURCES

If damping effect c is considered, the governing equations (10) can be extended as

$$L_{ij}(u_j) - c\dot{u}_i - \rho h\ddot{u}_i = q_i, \quad i,j = 1,2,3. \tag{29}$$

By defining the differential operator vectors

$$\mathbf{L}_i = \{L_{i1}, L_{i2}, L_{i3}\}, \tag{30}$$

where L_{ij} are given in equation (11), equation (29) can be further written as

$$\mathbf{L}_i\{u_1, u_2, u_3\}^{\mathrm{T}} - c\dot{u}_i - \rho h\ddot{u}_i = q_i, \quad i,j = 1,2,3. \tag{31}$$

The dynamic responses for the two pairs of the applied electric sources with 90° phase difference can be represented, respectively, by the summation of the mode components given in equation (28) as

$$u_i^{\varsigma}(\alpha_1, \alpha_2, t) = \sum_{k=1}^{3} U_{ik}^{\varsigma}(\alpha_1, \alpha_2)\eta_k^{\varsigma}(t), \quad \varsigma = s, c, \quad i = 1,2,3, \tag{32}$$

where $\eta_k^c(t)$ and $\eta_k^s(t)$ are the modal participation factors. Substituting equation (32) into equation (31) gives

$$\sum_{k=1}^{3}\left[\eta_k^{\varsigma}\mathbf{L}_i\{U_{1k}^{\varsigma}, U_{2k}^{\varsigma}, U_{3k}^{\varsigma}\}^{\mathrm{T}} - c\dot{\eta}_k^{\varsigma}U_{ik}^{\varsigma} - \rho h\ddot{\eta}_k^{\varsigma}U_{ik}^{\varsigma}\right] = q_i^{\varsigma}, \quad i = 1,2,3. \tag{33}$$

Since $U_{ik}^{\varsigma} \neq 0$, it is known from equation (17) that

$$\mathbf{L}_i\{U_{1k}^{\varsigma}, U_{2k}^{\varsigma}, U_{3k}^{\varsigma}\}^{\mathrm{T}} = -\rho h\omega_k^2 U_{ik}^{\varsigma}, \quad i = 1,2,3, \tag{34}$$

where ω_k is given by equation (25). Substituting equation (34) into equation (33) yields

$$\sum_{k=1}^{3}\left[(\ddot{\eta}_k^{\varsigma} + \frac{c}{\rho h}\dot{\eta}_k^{\varsigma} + \omega_k^2\eta_k^{\varsigma})U_{ik}^{\varsigma}\right] = -\frac{1}{\rho h}q_i^{\varsigma}, \quad i = 1,2,3. \tag{35}$$

Multiplying equation (35) by a modal shape U_{ip}^{ς} on both sides and integrating it over the cylinder surface, we have

$$\sum_{k=1}^{3}(\ddot{\eta}_k^{\varsigma}+\frac{c}{\rho h}\dot{\eta}_k^{\varsigma}+\omega_k^2\eta_k^{\varsigma})\int_0^L\int_0^{2\pi}\left(\sum_{i=1}^{3}U_{ik}^{\varsigma}U_{ip}^{\varsigma}\right)R\,\mathrm{d}\alpha_2\,\mathrm{d}\alpha_1$$
$$=-\frac{1}{\rho h}\int_0^L\int_0^{2\pi}\left(\sum_{i=1}^{3}q_i^{\varsigma}\right)U_{ip}^{\varsigma}R\,\mathrm{d}\alpha_2\,\mathrm{d}\alpha_1. \tag{36}$$

Using the orthogonal conditions of the modal shapes, the above expression can be simplified as

$$\ddot{\eta}_k^{\varsigma}+2\zeta_k\omega_k\dot{\eta}_k^{\varsigma}+\omega_k^2\eta_k^{\varsigma}=\hat{q}_k^{\varsigma},\quad k=1,2,3, \tag{37}$$

where

$$\hat{q}_k^{\varsigma}=-\frac{1}{\rho hN_k^{\varsigma}}\int_0^L\int_0^{2\pi}\left(\sum_{i=1}^{3}q_i^{\varsigma}U_{ik}^{\varsigma}\right)R\,\mathrm{d}\alpha_2\,\mathrm{d}\alpha_1,\quad N_k^{\varsigma}=\int_0^L\int_0^{2\pi}\left(\sum_{i=1}^{3}(U_{ik}^{\varsigma})^2\right)R\,\mathrm{d}\alpha_2\,\mathrm{d}\alpha_1, \tag{38}$$

and ζ_k is defined as the damping ratio given by

$$\zeta_k=\frac{c}{2\rho h\omega_k}. \tag{39}$$

For the applied electric sources shown in Figure 2, the exciting force components q_i^{ς} can be expressed as

$$\begin{aligned}q_i^c(\alpha_1,\alpha_2,t)&=Q_i^c(\alpha_1,\alpha_2)\cos\omega t=Q_i^c(\alpha_1,\alpha_2)\mathrm{e}^{\mathrm{j}\omega t},\\ q_i^s(\alpha_1,\alpha_2,t)&=Q_i^s(\alpha_1,\alpha_2)\sin\omega t=Q_i^s(\alpha_1,\alpha_2)\mathrm{e}^{\mathrm{j}(\pi/2-\omega t)},\end{aligned} \tag{40}$$

where $Q_i^c(\alpha_1,\alpha_2)$ and $Q_i^s(\alpha_1,\alpha_2)$ are the spatial part of the excitations, which can be obtained according to equation (12) as

$$\begin{aligned}Q_1^{\varsigma}(\alpha_1,\alpha_2)&=-e_{31}[\delta(\alpha_1)-\delta(\alpha_1-L)][\mathrm{H}(\alpha_2-\theta_{k1})-\mathrm{H}(\alpha_2-\theta_{k2})]V_0^{\varsigma},\\ Q_2^{\varsigma}(\alpha_1,\alpha_2)&=-\frac{e_{31}}{R}[\mathrm{H}(\alpha_1)-\mathrm{H}(\alpha_1-L)][\delta(\alpha_2-\theta_{k1})-\delta(\alpha_2-\theta_{k2})]V_0^{\varsigma},\\ Q_3^{\varsigma}(\alpha_1,\alpha_2)&=\frac{e_{31}}{R}[\mathrm{H}(\alpha_1)-\mathrm{H}(\alpha_1-L)][\mathrm{H}(\alpha_2-\theta_{k1})-\mathrm{H}(\alpha_2-\theta_{k2})]V_0^{\varsigma},\end{aligned} \tag{41}$$

and V_0^{ς} are defined according to the notations in equation (2) as

$$V_0^c=\begin{cases}V_0, & \theta_{11}<\alpha_2<\theta_{12},\\ -V_0, & \theta_{31}<\alpha_2<\theta_{32},\\ 0 & \text{for other } \alpha_2,\end{cases}\quad V_0^s=\begin{cases}V_0, & \theta_{21}<\alpha_2<\theta_{22},\\ -V_0, & \theta_{41}<\alpha_2<\theta_{42},\\ 0 & \text{for other } \alpha_2.\end{cases} \tag{42}$$

Therefore, equation (38) can be written as

$$\hat{q}_i^c(\alpha_1,\alpha_2,t)=\hat{Q}_i^c(\alpha_1,\alpha_2)\mathrm{e}^{\mathrm{j}\omega t},\qquad \hat{q}_i^s(\alpha_1,\alpha_2,t)=\hat{Q}_i^s(\alpha_1,\alpha_2)\mathrm{e}^{\mathrm{j}(\pi/2-\omega t)}, \tag{43}$$

where

$$\hat{Q}_k^{\varsigma}=-\frac{1}{\rho hN_k^{\varsigma}}\int_0^L\int_0^{2\pi}\left(\sum_{i=1}^{3}Q_i^{\varsigma}U_{ik}^{\varsigma}\right)R\,\mathrm{d}\alpha_2\,\mathrm{d}\alpha_1. \tag{44}$$

Substituting equation (40) into equation (37), the steady state responses can be obtained in the form as

$$\eta_k^c(t) = \frac{\hat{Q}_k^c}{\omega_k^2} \mathrm{H}_k(\omega) \mathrm{e}^{\mathrm{j}\omega t} = \Lambda_k^c \mathrm{e}^{\mathrm{j}(\omega t - \phi_k)},$$
$$\eta_k^s(t) = \frac{\hat{Q}_k^s}{\omega_k^2} \overline{\mathrm{H}_k(\omega)} \mathrm{e}^{\mathrm{j}(\pi/2 - \omega t)} = \Lambda_k^s \mathrm{e}^{\mathrm{j}(\pi/2 - \omega t + \phi_k)}, \tag{45}$$

where

$$\mathrm{H}_k(\omega) = \frac{1}{1 - (\omega/\omega_k)^2 + \mathrm{j}2\zeta_k \omega/\omega_k} = |\mathrm{H}_k(\omega)| \mathrm{e}^{-\mathrm{j}\phi_k}, \quad \phi_k = \arctan \frac{2\zeta_k \omega/\omega_k}{1 - (\omega/\omega_k)^2},$$
$$|\mathrm{H}_k(\omega)| = \frac{1}{\sqrt{\left[1 - (\omega/\omega_k)^2\right]^2 + (2\zeta_k \omega/\omega_k)^2}}, \tag{46}$$

and

$$\Lambda_k^c = \frac{\hat{Q}_k^c}{\omega_k^2} |\mathrm{H}_k(\omega)|, \quad \Lambda_k^s = \frac{\hat{Q}_k^s}{\omega_k^2} |\mathrm{H}_k(\omega)|. \tag{47}$$

We now determine the expressions of $\hat{Q}_k^{\varsigma}$ in equation (44). First, we determine N_k^{ς}. Substituting the relevant modal components in equation (28) into the second expression of equation (38), we obtain

$$N_k = N_k^c = N_k^s = \pi R \left[R^2 \bar{C}_{1k}^2 \frac{\int_0^L (dW/d\alpha_1)^2 \, \mathrm{d}\alpha_1}{\int_0^L W^2 \, \mathrm{d}\alpha_1} + \bar{C}_{2k}^2 + 1 \right] \int_0^L W^2 \, \mathrm{d}\alpha_1. \tag{48}$$

Therefore, by substituting equations (28), (41) and (42) into equation (44), the explicit expressions of $\hat{Q}_k^{\varsigma}$ can be obtained as

$$\hat{Q}_k = \hat{Q}_k^c = \hat{Q}_k^s = -\frac{2\sqrt{2} e_{31}}{\rho h N_k} \left[R^2 \bar{C}_{1k} \left(\frac{\mathrm{d}W(0)}{\mathrm{d}\alpha_1} - \frac{\mathrm{d}W(L)}{\mathrm{d}\alpha_1} \right) + (1 - \bar{C}_{2k}) \int_0^L W \, \mathrm{d}\alpha_1 \right] V_0. \tag{49}$$

Since $\hat{Q}_k^c = \hat{Q}_k^s$, it is known from equation (47) that $\Lambda_k^c = \Lambda_k^s$, which can be simply denoted by Λ_k. Thus, from equations (45) and (32), we have

$$u_i^c(\alpha_1, \alpha_2, t) = \sum_{k=1}^3 \Lambda_k U_{ik}^c(\alpha_1, \alpha_2) \cos(\omega t - \phi_k),$$
$$u_i^s(\alpha_1, \alpha_2, t) = \sum_{k=1}^3 \Lambda_k U_{ik}^s(\alpha_1, \alpha_2) \sin(\omega t - \phi_k). \tag{50}$$

Substituting equations (50) and (28) into equation (16), the steady state response of the cylinder transducer excited by the electric sources shown in Figure 2 are obtained as

$$u_1(\alpha_1, \alpha_2, t) = -R \frac{\mathrm{d}W}{\mathrm{d}\alpha_1} \sum_{k=1}^3 \bar{C}_{1k} \Lambda_k \cos(\omega t - \phi_k - \alpha_2),$$
$$u_2(\alpha_1, \alpha_2, t) = W \sum_{k=1}^3 \bar{C}_{2k} \Lambda_k \sin(\omega t - \phi_k - \alpha_2),$$
$$u_3(\alpha_1, \alpha_2, t) = W \sum_{k=1}^3 \Lambda_k \cos(\omega t - \phi_k - \alpha_2). \tag{51}$$

If the applied frequency is very close to the bending frequency, say ω_1, equation (51) can be further simplified as

$$u_1(\alpha_1, \alpha_2, t) = -R \bar{C}_{11} \Lambda_1 \frac{dW}{d\alpha_1} \cos(\omega t - \phi_1 - \alpha_2),$$
$$u_2(\alpha_1, \alpha_2, t) = \bar{C}_{21} \Lambda_1 W \sin(\omega t - \phi_1 - \alpha_2),$$
$$u_3(\alpha_1, \alpha_2, t) = \Lambda_1 W \cos(\omega t - \phi_1 - \alpha_2). \tag{52}$$

By comparing equation (52) with equation (13), it is found that the amplitude components of the three displacement variables have been determined, which is impossible to be determined by beam theory. Substituting equation (51) into equations (5)–(7), the strain and stress components can be obtained, which are listed in Appendix A.

4. ELECTROMECHANICAL COUPLING EFFECTS

For the considered piezoelectric cylindrical shell with a hexagonal symmetrical structure, the electric displacement component along the thickness direction, D_3, is given by

$$D_3 = e_{31}S_{11} + e_{31}S_{22} + \varepsilon_{33}E_3, \tag{53}$$

where ε_{33} is the dielectric permittivity. Substituting equation (A2) into equation (53), we have

$$\begin{aligned} D_3 = {} & \varepsilon_{33}E_3 + e_{31}\sum_{k=1}^{3}\left[-(R\bar{C}_{1k}+\alpha_3)\frac{\mathrm{d}^2W}{\mathrm{d}\alpha_1^2}\right. \\ & \left.+\frac{1}{R}(1-\bar{C}_{2k})\left(1+\frac{\alpha_3}{R}\right)W\right]\Lambda_k\cos(\omega t-\phi_k-\alpha_2). \end{aligned} \tag{54}$$

It is noted that D_3 is the summation of the two electric displacements D_3^c and D_3^s, which are induced by the two pairs of the voltages with 90^0 phase difference as shown in Figure 2. Therefore, we have

$$\begin{aligned} D_3^c = {} & -\varepsilon_{33}\frac{V_0^c}{h}\cos\omega t + e_{31}\sum_{k=1}^{3}\left[-(R\bar{C}_{1k}+\alpha_3)\frac{\mathrm{d}^2W}{\mathrm{d}\alpha_1^2}\right. \\ & \left.+\frac{1}{R}(1-\bar{C}_{2k})(1+\frac{\alpha_3}{R})W\right]\Lambda_k\cos\alpha_2\cos(\omega t-\phi_k), \\ D_3^s = {} & -\varepsilon_{33}\frac{V_0^s}{h}\sin\omega t + e_{31}\sum_{k=1}^{3}\left[-(R\bar{C}_{1k}+\alpha_3)\frac{\mathrm{d}^2W}{\mathrm{d}\alpha_1^2}\right. \\ & \left.+\frac{1}{R}(1-\bar{C}_{2k})\left(1+\frac{\alpha_3}{R}\right)W\right]\Lambda_k\sin\alpha_2\sin(\omega t-\phi_k), \end{aligned} \tag{55}$$

where V_0^c and V_0^s are defined in equation (42). Integrating either one of the expressions in equations (55) over the electrode surfaces, we obtain the charge in the electrodes:

$$\begin{aligned} Q = {} & \int_{\Omega_0} D_3^c\,\mathrm{d}\Omega = \int_0^L\left[\left(\int_{\theta_{11}}^{\theta_{12}}+\int_{\theta_{31}}^{\theta_{32}}\right)D_3^cR\,\mathrm{d}\alpha_2\right]\mathrm{d}\alpha_1 \\ = {} & -\varepsilon_{33}\frac{\pi RL}{h}V_0\cos\omega t + 2\sqrt{2}e_{31}\sum_{k=1}^{3}\left[-R^2\left(\bar{C}_{1k}+\frac{h}{2R}\right)\left(\left.\frac{\mathrm{d}W}{\mathrm{d}\alpha_1}\right|_{\alpha_1=L}-\left.\frac{\mathrm{d}W}{\mathrm{d}\alpha_1}\right|_{\alpha_1=0}\right)\right. \\ & \left.+(1-\bar{C}_{2k})\left(1+\frac{h}{2R}\right)\int_0^L W\,\mathrm{d}\alpha_1\right]\Lambda_k\cos(\omega t-\phi_k), \end{aligned} \tag{56}$$

Substituting equations (47)–(49) into equation (56), we obtain

$$Q = CV_0\mathrm{e}^{\mathrm{j}\omega t} = (C_0+C_m)V_0\mathrm{e}^{\mathrm{j}\omega t}, \tag{57}$$

where C is the dynamic capacitance of the piezocylinder given by

$$C_0 = \frac{\pi RL}{h}\varepsilon_{33},$$

$$C_m = \frac{8e_{31}^2}{\rho h}\sum_{k=1}^{3}\frac{1}{N_k\omega_k^2}\left[R^2\left(\bar{C}_{1k}+\frac{h}{2R}\right)\left(\left.\frac{\mathrm{d}W}{\mathrm{d}\alpha_1}\right|_{\alpha_1=0}-\left.\frac{\mathrm{d}W}{\mathrm{d}\alpha_1}\right|_{\alpha_1=L}\right)\right.$$
$$\left.+(1-\bar{C}_{2k})\left(1+\frac{h}{2R}\right)\int_0^L W\,\mathrm{d}\alpha_1\right]^2 \mathrm{H}_k(\omega). \tag{58}$$

If the frequency of the applied dynamic voltage ω is very close to the bending frequency ω_1, and the damping effect is not considered, C_m can be further reduced to for $h/2R << 1$:

$$C_m = \frac{8e_{31}^2}{\rho h N_1}\left[R^2\bar{C}_{11}\left(\left.\frac{dW}{d\alpha_1}\right|_{\alpha_1=0}-\left.\frac{dW}{d\alpha_1}\right|_{\alpha_1=L}\right)+(1-\bar{C}_{21}\int_0^L W\,\mathrm{d}\alpha_1\right]^2\frac{1}{\omega_1^2-\omega^2}. \tag{59}$$

The current flowing into the electrode surfaces is calculated as

$$I = \frac{\partial Q}{\partial t} = \mathrm{j}\omega Q, \tag{60}$$

and the admittance is given by

$$Y = \frac{I}{V_0\mathrm{e}^{\mathrm{j}\omega t}} = \mathrm{j}\omega C. \tag{61}$$

According to the definitions of resonance and antiresonance, the resonant frequency can be determined by letting $Y \to \infty$, and the antiresonant frequency by $Y = 0$. Therefore, it can be found from equations (61) and (59) that the resonant frequency ω_r is equal to the bending frequency ω_1, and the related antiresonant frequency ω_a is obtained as

$$\omega_a^2 = \omega_1^2 + \frac{8}{\pi RL\rho N_1}\frac{e_{31}^2}{\varepsilon_{33}}\left[R^2\bar{C}_{11}\left(\left.\frac{\mathrm{d}W}{\mathrm{d}\alpha_1}\right|_{\alpha_1=0}-\left.\frac{\mathrm{d}W}{\mathrm{d}\alpha_1}\right|_{\alpha_1=L}\right)+(1-\bar{C}_{21})\int_0^L W\,\mathrm{d}\alpha_1\right]^2. \tag{62}$$

With one of the definitions for electromechanical coupling coefficient k_{eff} defined by

$$k_{eff}^2 = \frac{\omega_a^2-\omega_r^2}{\omega_a^2}, \tag{63}$$

the electromechanical coupling coefficients of the cylinder transducer at the bending resonance mode can be estimated from relation (63).

To estimate the performance of a piezoelectric ultrasonic motor, a parameter called force factor A is introduced [6]. It is defined as the force created when a unit voltage is applied, or the current generated when unit velocity is imparted to the ceramic body. We now determine the force factor of the cylinder transducer under bending vibration mode.

From equations (60), (57), and (59), it is known that the displacement current I_m is calculated by

$$I_m = \mathrm{j}\omega C_m V_0\mathrm{e}^{\mathrm{j}\omega t}$$

$$= \mathrm{j}\omega\frac{8e_{31}^2}{\rho h N_1}\left[R^2\bar{C}_{11}\left(\left.\frac{\mathrm{d}W}{\mathrm{d}\alpha_1}\right|_{\alpha_1=0}-\left.\frac{\mathrm{d}W}{\mathrm{d}\alpha_1}\right|_{\alpha_1=L}\right)+(1-\bar{C}_{21})\int_0^L W\,\mathrm{d}\alpha_1\right]^2\frac{V_0\mathrm{e}^{\mathrm{j}\omega t}}{\omega_1^2-\omega^2}. \tag{64}$$

The vibration velocity of the transducer at the end surface, under the bending vibration mode, can be calculated from the expression in equation (52) as

$$v = \left.\frac{\partial u_3}{\partial t}\right|_{\alpha_1=L\ \alpha_2=0} = \mathrm{j}\omega W(L)\hat{Q}_1 \frac{1}{\omega_1^2 - \omega^2} \mathrm{e}^{\mathrm{i}\omega t}$$

$$= -\mathrm{j}\omega W(L)\frac{2\sqrt{2}e_{31}}{\rho h N_1}\left[R^2\bar{C}_{11}\left(\left.\frac{\mathrm{d}W}{\mathrm{d}\alpha_1}\right|_{\alpha_1=0} - \left.\frac{\mathrm{d}W}{\mathrm{d}\alpha_1}\right|_{\alpha_1=L}\right) + (1-\bar{C}_{21})\int_0^L W\,\mathrm{d}\alpha_1\right]\frac{V_0\mathrm{e}^{\mathrm{i}\omega t}}{\omega_1^2 - \omega^2}. \quad (65)$$

Therefore, the force factor A is obtained as

$$A = \left|\frac{I_m}{v}\right| = \left|\frac{2\sqrt{2}e_{31}}{W(L)}\left[R^2\bar{C}_{11}\left(\left.\frac{\mathrm{d}W}{\mathrm{d}\alpha_1}\right|_{\alpha_1=0} - \left.\frac{\mathrm{d}W}{\mathrm{d}\alpha_1}\right|_{\alpha_1=L}\right) + (1-\bar{C}_{21})\int_0^L W\,\mathrm{d}\alpha_1\right]\right|. \quad (66)$$

With the force factor, the performance of the cylindrical micromotors can be estimated.

5. NUMERICAL EXAMPLES AND DISCUSSIONS

In the above derivations, the displacements of the cylindrical transducer are assumed to have the form shown in equation (13), in which W is the mode shape of a transversely vibrating beam of the same boundary conditions with the cylinder. Since the cylinder transducer is considered to have free–free boundary conditions, the first order free–free beam bending mode is used. By substituting it into the above expressions, the relevant results can be further simplified.

If the transducer is a uniform sized thin wall cylinder, the mode shape function of uniform free–free beam is used, which is given by

$$W\left(\frac{\eta}{L}\alpha_1\right) = \cosh\frac{\eta}{L}\alpha_1 + \cos\frac{\eta}{L}\alpha_1 - \frac{\cosh\eta - \cos\eta}{\sinh\eta - \sin\eta}\left(\sinh\frac{\eta}{L}\alpha_1 + \sin\frac{\eta}{L}\alpha_1\right), \quad (67)$$

where η is the eigenvalue of the free–free beam. For the first beam mode, $\eta = 4{\cdot}730$, we have

$$\int_0^L W\,\mathrm{d}\alpha_1 = 0, \quad \int_0^L (\mathrm{d}W/\mathrm{d}\alpha_1)^2 \quad \mathrm{d}\alpha_1 = 49{\cdot}47965/L, \quad \int_0^L W^2\,\mathrm{d}\alpha_1 = L,$$

$$W(0) = W(L) = 2, \quad W'(L) = -W'(0) = 9{\cdot}29447/L. \quad (68)$$

Therefore, the amplitude components $\hat{Q}_k$ in equation (49) are simplified to

$$\hat{Q}_k = \frac{52{\cdot}5827R\bar{C}_{1k}e_{31}}{\pi h\rho[49{\cdot}4846R^2\bar{C}_{1k}^2 + L^2(\bar{C}_{2k}^2 + 1)]}V_0, \quad (69)$$

and the force factor A in equation (66) is reduced to

$$A = \frac{26{\cdot}2887R^2\bar{C}_{11}e_{31}}{L}. \quad (70)$$

As an example, the vibration characteristics of a piezoelectric tube are estimated with the proposed method. The material properties of the tube are given by Young's modulus $E = 8{\cdot}65 \times 10^{10}$ Pa; Density $\rho = 7{\cdot}54 \times 10^3$ kg/m^3; the Poisson ratio $\mu = 0{\cdot}29$; and piezoelectric strain coefficient $d_{31} = -0{\cdot}45$ m/V. The geometry parameters of the

tube are, outer diameter $D_o = 3{\cdot}2\,\text{mm}$; inner diameter $D_i = 2{\cdot}4\,\text{mm}$; and length $L = 10{\cdot}0\,\text{mm}$. The measured first bending frequency is $f_1 = 87\,\text{kHz}$. According to the data given above, the bending frequency estimated according to the beam theory [1] is $f_1 = 76\,\text{kHz}$. It is much lower than the measured result. The calculated frequency components f_i and the non-dimensional amplitude ratios C_{ij} according to the present method are listed in Table 1.

In the table, the lowest frequency f_1 is associated with the bending mode, f_2 and f_3 are associated with circumferential and longitudinal modes respectively. It is seen that f_2 and f_3 are one order higher than the magnitude of f_1, and the corresponding modes are higher modes comparing with the bending mode. Therefore, it is not difficult to excite the required bending mode with the applied frequency close to f_1. Comparing with the measured bending frequency of the tube, the theoretical estimation by the method is satisfied, and is better than the result obtained by the beam theory. With the frequencies and the corresponding amplitude ratios obtained, the displacements can be calculated by equation (52) and the force factor by equation (70).

To verify the validity of the present method by more examples, the data of three types of stator transducers given in reference [7] are used for the calculations. The material properties and the transducer dimensions are listed in Table 2.

The measured bending frequencies for types 1–3 transducers are 227, 110, and 72 kHz respectively. The calculated results based on the present method are given in Table 3. The bending frequencies of the transducers obtained by the beam theory [1] are also listed for comparisons. It can be seen that for the transducers of types 1 and 3, the calculated bending frequencies based on the present method are better than that obtained by the beam theory, while for type 2, the two methods provide similar estimations. It is due to the

TABLE 1

Frequencies and amplitude ratios of a piezoelectric tube

$E = 8{\cdot}65 \times 10^{10}\,\text{Pa}$, $\rho = 7{\cdot}54 \times 10^3\,\text{kg/m}^3$, $\mu = 0{\cdot}29$, $h = 0{\cdot}4\,\text{mm}$, $R = 1{\cdot}4\,\text{mm}$, $L = 10\,\text{mm}$

f_1 (kHz)	$\bar{C}_{11}$	$\bar{C}_{21}$	$\bar{C}_{31}$
82·4	0·494	1·025	1·0
f_2 (kHz)	$\bar{C}_{12}$	$\bar{C}_{22}$	$\bar{C}_{32}$
602·0	0·702	−1·112	1·0
f_3 (kHz)	$\bar{C}_{13}$	$\bar{C}_{23}$	$\bar{C}_{33}$
334·4	−3·844	−0·164	1·0

TABLE 2

Dimensions of three types of stator transducers

$E = 1{\cdot}1 \times 10^{11}\,\text{N/m}^2$ $\rho = 4{\cdot}51 \times 10^3\,\text{kg/m}^3$, $\mu = 0{\cdot}3$

	h (mm)	R (mm)	L (mm)
Type 1	0·1	0·65	5
Type 2	0·25	1.075	10
Type 3	0·1	0·65	10

TABLE 3

Calculated frequencies and amplitude ratios

	f_1(kHz) [1]	f_1 (kHz)	$\bar{C}_{11}$	$\bar{C}_{21}$	f_2 (kHz)	$\bar{C}_{12}$	$\bar{C}_{22}$	f_3 (kHz)	$\bar{C}_{13}$	$\bar{C}_{23}$
Type 1	**221**	**229·5**	0·530	1·028	1877·6	0·696	−1·108	1013·9	−4·337	−0·128
Type 2	**104**	**103·8**	0·628	1·032	1120·2	0·653	−1·072	572·0	−6·044	0·019
Type 3	**74·5**	**72·5**	0·823	1·020	1814·0	0·603	−1·026	832·1	−14·83	0·150

reason that the geometries of types 1 and 3 transducers are closer to thin shell structures than that of type 2 transducer. Therefore, the present method based on thin shell theory provides better estimations for types 1 and 3 transducers than the estimations for the transducers of type 2 and previous example. By comparing the results obtained by the present method and the beam theory, it is seen that the present method generally provides better estimations.

From Table 3, we can also find that the non-dimensional amplitude ratio $\bar{C}_{21}$ is close to unit for all types of the transducers. By referring to the mode shape and displacement expressions (28) and (52), it physically means that for the bending vibration, the difference of the maximum amplitudes for the circumferential and radial components, u_2 and u_3, is very small. This is in agreement with the approximate analysis in reference [2] based on beam bending mode. However, the ratio $\bar{C}_{11}$ cannot be determined there.

With the obtained amplitude ratio $\bar{C}$, the force factor A can be predicated according to equation (70). Reference [7] also gives an expression to predicate the force factor, which can be simplified as

$$A = \frac{13{\cdot}1445R^2 e_{31}}{L}. \tag{71}$$

Comparing with the expression, it is seen that the force factor given in equation (70) has one more parameter, $\bar{C}_{11}$, which cannot be determined with the one-dimensional beam theory. With the piezoelectric coefficient e_{31} to be $-0{\cdot}57\,\mathrm{C/m^2}$, the force factors for the cylinder-type stator transducers are estimated by Equations (70) and (71) respectively. The results are given in the Table 4, in which the measured values in reference [7] are also listed for reference. It can be seen that the overall estimated results by equation (70) are satisfied. Furthermore, the maximum output force F_{max} can be estimated by the relation AV_0 and the maximum output torque by AV_0R, where V_0 is the amplitude of the applied voltage.

TABLE 4

Estimated force factors

$e_{31} = -0{\cdot}57$ (C/m^2)	A (mN/V)		
	Reference [7]	Equation (70)	Equation (71)
Type 1	0·61	0·67	0·63
Type 2	1·1	1·09	0·87
Type 3	0·44	0·52	0·32

The rotating speed of the cylindrical motor can be estimated by the relation $v = \partial u_2/\partial t|_{\max}$ [2]. By substituting the expression of u_2 from equation (52), we have

$$v = \bar{C}_2 \Lambda W(L)\omega = \bar{C}_2 W(L)\omega \frac{\hat{Q}}{\omega^2}|\mathrm{H}(\omega)|$$

$$= \frac{\bar{C}_2 W(L)\omega}{\omega^2 \sqrt{\left[1-(\omega/\omega)^2\right]^2 + (2\zeta\omega/\omega)^2}} \frac{52{\cdot}5827 R\bar{C}e_3}{\pi h\rho[49{\cdot}4846R^2\bar{C}^2 + L^2(\bar{C}_2^2+1)]} V_0. \tag{72}$$

It can be seen that the rotating speed of this kind of motors is indeed linearly proportional to the amplitude of input voltage as measured in reference [7]. To estimate the speed with equation (72), the structure damping of the transducer ζ_1 should be known at first through some way.

6. CONCLUDING REMARKS

In the present paper, the vibration of the cylindrical stator transducer induced by applied voltage is studied based on shell theory. According to the motion principle of the transducer, the displacement components are properly assumed so that a one-wavelength travelling wave motion, as shown in Figure 1, can be generated by the displacements. Therefore, the displacement components can be expressed by the superposition of two same vibration modes but perpendicular to each other, which are excited by two pairs of electrical sources with 90° phase difference respectively. The properties of the vibration modes, such as mode frequencies, amplitude ratios of the mode shapes, are determined following the Galerkin method. The response of the transducer under the four electric sources with 90° phase difference are then obtained by the modal summation method. With the results, the performance of the transducer under the electric sources can be estimated.

Since the vibration of the transducer is analyzed based on more reasonable elastic cylinder model, and the applied electric forces are also well modelled, the present work provides a generalized theoretical modelling on the dynamical movement of the transducer. The numerical examples show that the results obtained by the model are satisfied. This study is a modification of the one-dimensional beam model used in the literature for the analysis of this kind of the stator transducers. For further study, the overall dynamical analysis of the cylindrical micromotors, including stator transducer, rotors and preload, should be considered. It would be more complicated because more factors, such as contact forces, frictional characteristics, contact surface properties, and temperature effect, will be involved.

REFERENCES

1. T. Morita, M. Kurosawa and T. Higuchi 1995 *Sensors and Actuators A* **50**, 75–80. An ultrasonic micromotor using a bending cylindrical transducer based on PZT thin film.
2. P. Lu, K. H. Lee, S. P. Lim and W. Z. Lin 2001 *Sensors and Actuators A* **87**, 194–197. A kinematic analysis of cylindrical ultrasonic micromotors.
3. C.-K. Lee 1992 *Intelligent Structural Systems* (H. S. Tzou and G. L. Anderson editors). 75–167. Dordrecht: Kluwer Academic Publishers, Piezoelectric laminates: theory and experiments for distributed sensors and actuators.
4. H. S. Tzou 1993 *Piezoelectric Shells: Distributed Sensing and Control of Continua*. Dordrecht: Kluwer Academic Publishers.

5. W. Soedel 1993 *Vibrations of Shells and Plates*. New York: Marcel Dekker, second edition.
6. T. Sashida and T. Kenjo 1993 *An Introduction to Ultrasonic Motors*. Oxford: Oxford University Press.
7. T. Morita, M. Kurosawa and T. Higuchi 2000 *Sensors and Actuators A* **83**, 225–230. A cylindrical shaped micro ultrasonic motor utilizing PZT thin film (1.4 mm in diameter and 5.0 mm long stator transducer).

APPENDIX A

Substituting equation (51) into equations (5)–(7), we have the strain components

$$\begin{aligned}
S_{11}^0 &= \frac{\partial u_1}{\partial \alpha_1} = -R\frac{\mathrm{d}^2 W}{\mathrm{d}\alpha_1^2}\sum_{k=1}^{3}\bar{C}_{1k}\Lambda_k \cos(\omega t - \phi_k - \alpha_2),\\
S_{22}^0 &= \frac{1}{R}\frac{\partial u_2}{\partial \alpha_2} + \frac{u_3}{R} = \frac{1}{R}W\sum_{k=1}^{3}(1-\bar{C}_{2k})\Lambda_k \cos(\omega t - \phi_k - \alpha_2),\\
S_{12}^0 &= \frac{1}{R}\frac{\partial u_1}{\partial \alpha_2} + \frac{\partial u_2}{\partial \alpha_1} = \frac{dW}{d\alpha_1}\sum_{k=1}^{3}(\bar{C}_{2k}-\bar{C}_{1k})\Lambda_k \sin(\omega t - \phi_k - \alpha_2),
\end{aligned} \tag{A1}$$

$$\begin{aligned}
\kappa_{11} &= -\frac{\partial^2 u_3}{\partial \alpha_1^2} = -\frac{d^2 W}{d\alpha_1^2}\sum_{k=1}^{3}\Lambda_k \cos(\omega t - \phi_k - \alpha_2),\\
\kappa_{22} &= \frac{1}{R^2}\left(\frac{\partial u_2}{\partial \alpha_2} - \frac{\partial^2 u_3}{\partial \alpha_2^2}\right) = \frac{1}{R^2}W\sum_{k=1}^{3}(1-\bar{C}_{2k})\Lambda_k \cos(\omega t - \phi_k - \alpha_2),\\
\kappa_{12} &= \frac{1}{R}\left(\frac{\partial u_2}{\partial \alpha_1} - 2\frac{\partial^2 u_3}{\partial \alpha_1 \partial \alpha_2}\right) = \frac{1}{R}\frac{\mathrm{d}W}{\mathrm{d}\alpha_1}\sum_{k=1}^{3}(\bar{C}_{2k}-2)\Lambda_k \sin(\omega t - \phi_k - \alpha_2),
\end{aligned} \tag{A2}$$

and

$$\begin{aligned}
S_{11} &= S_{11}^0 + \alpha_3\kappa_{11} = -\frac{\mathrm{d}^2 W}{\mathrm{d}\alpha_1^2}\sum_{k=1}^{3}(R\bar{C}_{1k}+\alpha_3)\Lambda_k \cos(\omega t - \phi_k - \alpha_2),\\
S_{22} &= S_{22}^0 + \alpha_3\kappa_{22} = \frac{1}{R}\left(1+\frac{\alpha_3}{R}\right)W\sum_{k=1}^{3}(1-\bar{C}_{2k})\Lambda_k \cos(\omega t - \phi_k - \alpha_2),\\
S_{12} &= S_{12}^0 + \alpha_3\kappa_{12} = \frac{\mathrm{d}W}{\mathrm{d}\alpha_1}\sum_{k=1}^{3}\left[\left(1+\frac{\alpha_3}{R}\right)\bar{C}_{2k} - \bar{C}_{1k} - 2\right]\Lambda_k \sin(\omega t - \phi_k - \alpha_2).
\end{aligned} \tag{A3}$$

The mechanical membrane forces N_{ij}^m and bending moments M_{ij}^m are obtained as

$$\begin{aligned}
N_{11}^m &= K(S_{11}^0 + \mu S_{22}^0) = K\sum_{k=1}^{3}\left[-R\bar{C}_{1k}\frac{\mathrm{d}^2 W}{\mathrm{d}\alpha_1^2} + \frac{\mu}{R}(1-\bar{C}_{2k})W\right]\Lambda_k \cos(\omega t - \phi_k - \alpha_2),\\
N_{22}^m &= K(S_{22}^0 + \mu S_{11}^0) = K\sum_{k=1}^{3}\left[\frac{1}{R}(1-\bar{C}_{2k})W - \mu R\bar{C}_{1k}\frac{\mathrm{d}^2 W}{\mathrm{d}\alpha_1^2}\right]\Lambda_k \cos(\omega t - \phi_k - \alpha_2),\\
N_{12}^m &= \frac{K(1-\mu)}{2}S_{12}^0 = \frac{K(1-\mu)}{2}\frac{\mathrm{d}W}{\mathrm{d}\alpha_1}\sum_{k=1}^{3}(\bar{C}_{2k}-\bar{C}_{1k})\Lambda_k \sin(\omega t - \phi_k - \alpha_2),
\end{aligned} \tag{A4}$$

and

$$M_{11}^m = D(\kappa_{11} + \mu\kappa_{22}) = D\sum_{k=1}^{3}\left[-\frac{\mathrm{d}^2 W}{\mathrm{d}\alpha_1^2} + \frac{\mu}{R^2}(1 - \bar{C}_{2k})W\right]\Lambda_k \cos(\omega t - \phi_k - \alpha_2),$$

$$M_{22}^m = D(\kappa_{22} + \mu\kappa_{11}) = D\sum_{k=1}^{3}\left[\frac{1}{R^2}(1 - \bar{C}_{2k})W - \mu\frac{\mathrm{d}^2 W}{\mathrm{d}\alpha_1^2}\right]\Lambda_k \cos(\omega t - \phi_k - \alpha_2),$$

$$M_{12}^m = \frac{D(1-\mu)}{2}\kappa_{12} = \frac{D(1-\mu)}{2R}\frac{\mathrm{d}W}{\mathrm{d}\alpha_1}\sum_{k=1}^{3}(\bar{C}_{2k} - 2)\Lambda_k \sin(\omega t - \phi_k - \alpha_2). \tag{A5}$$